Stem Cell Reports, Volume *4*

Supplemental Information

Models of Breast Morphogenesis Based on Localization of Stem Cells in the Developing Mammary Lobule

Gabriella Honeth, Tommaso Schiavinotto, Federico Vaggi, Rebecca Marlow, Tokuwa Kanno, Ireneusz Shinomiya, Sara Lombardi, Bharath Buchupalli, Rosalind Graham, Patrycja Gazinska, Vernie Ramalingam, Joy Burchell, Anand D. Purushotham, Sarah E. Pinder, Attila Csikasz-Nagy, and Gabriela Dontu

A

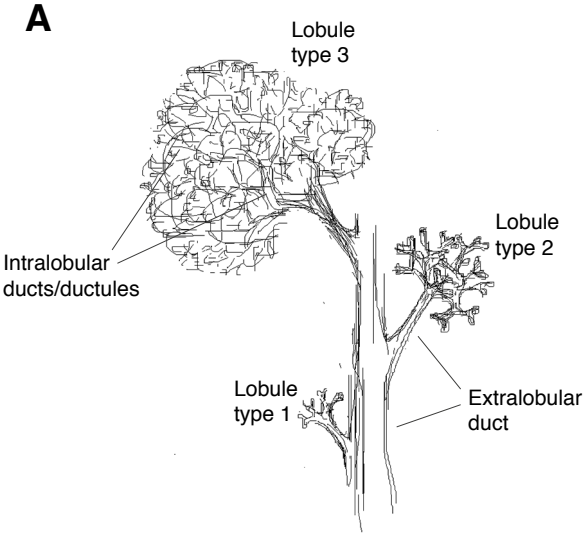

B

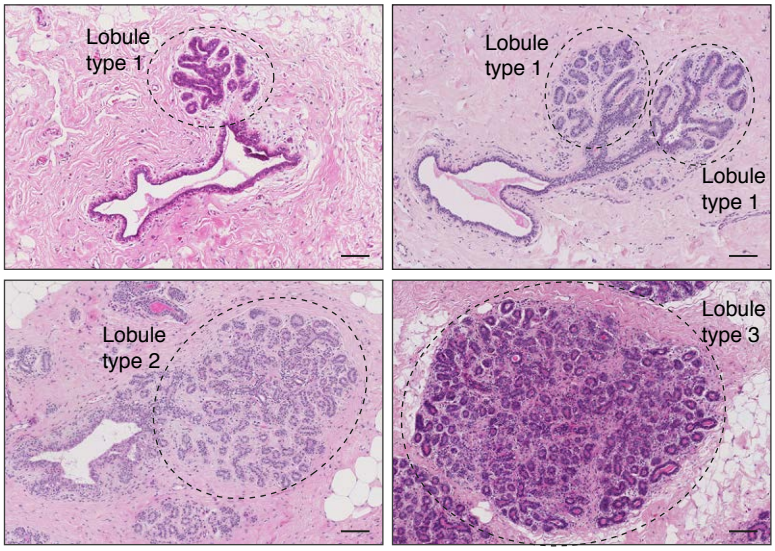

C

	Fate 1	Fate 2
A. Type of SC division	Asymmetric self-renewal (A1)	Differentiation (A2)
B. Rate of SC division	Low (B1)	High (B2
C. Orientation of SC	Distal (C1)	Proximal (C2)

D

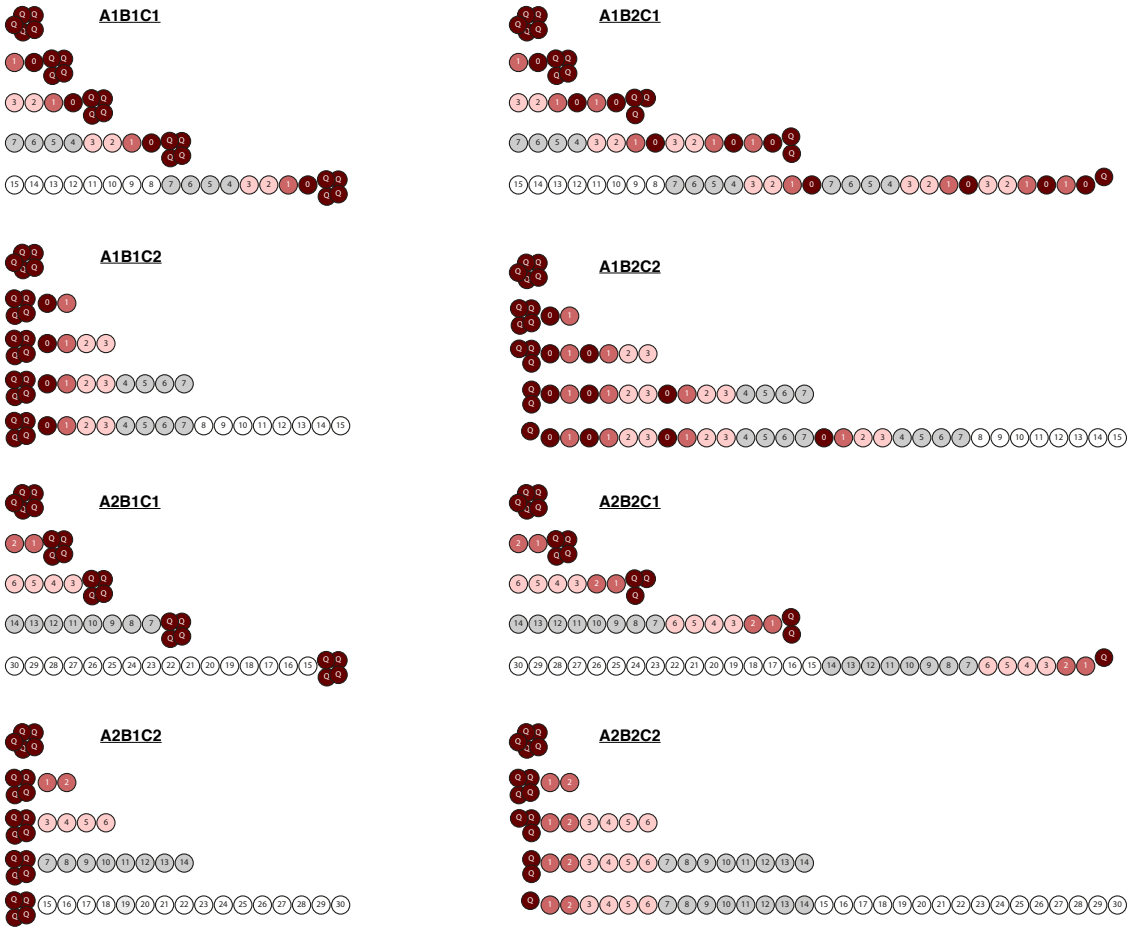

E

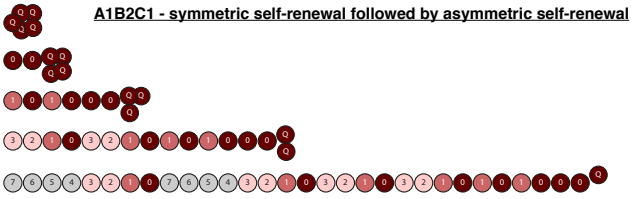

F

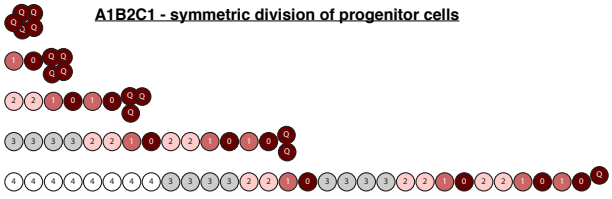

FIGURE S1

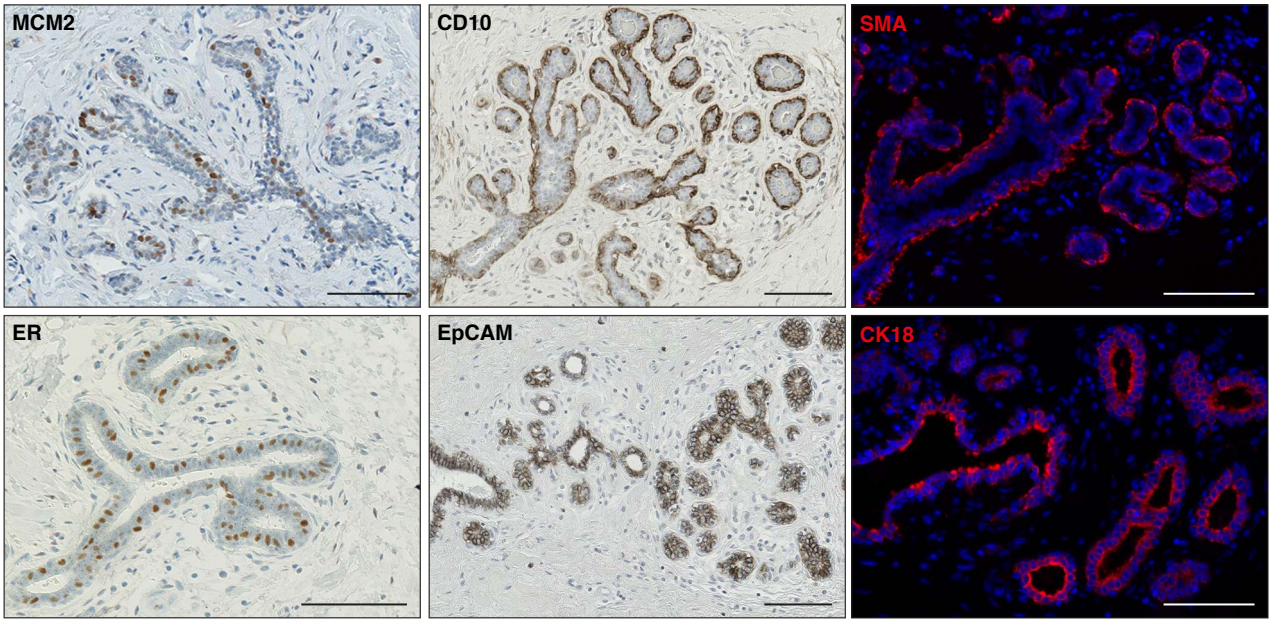

FIGURE S2

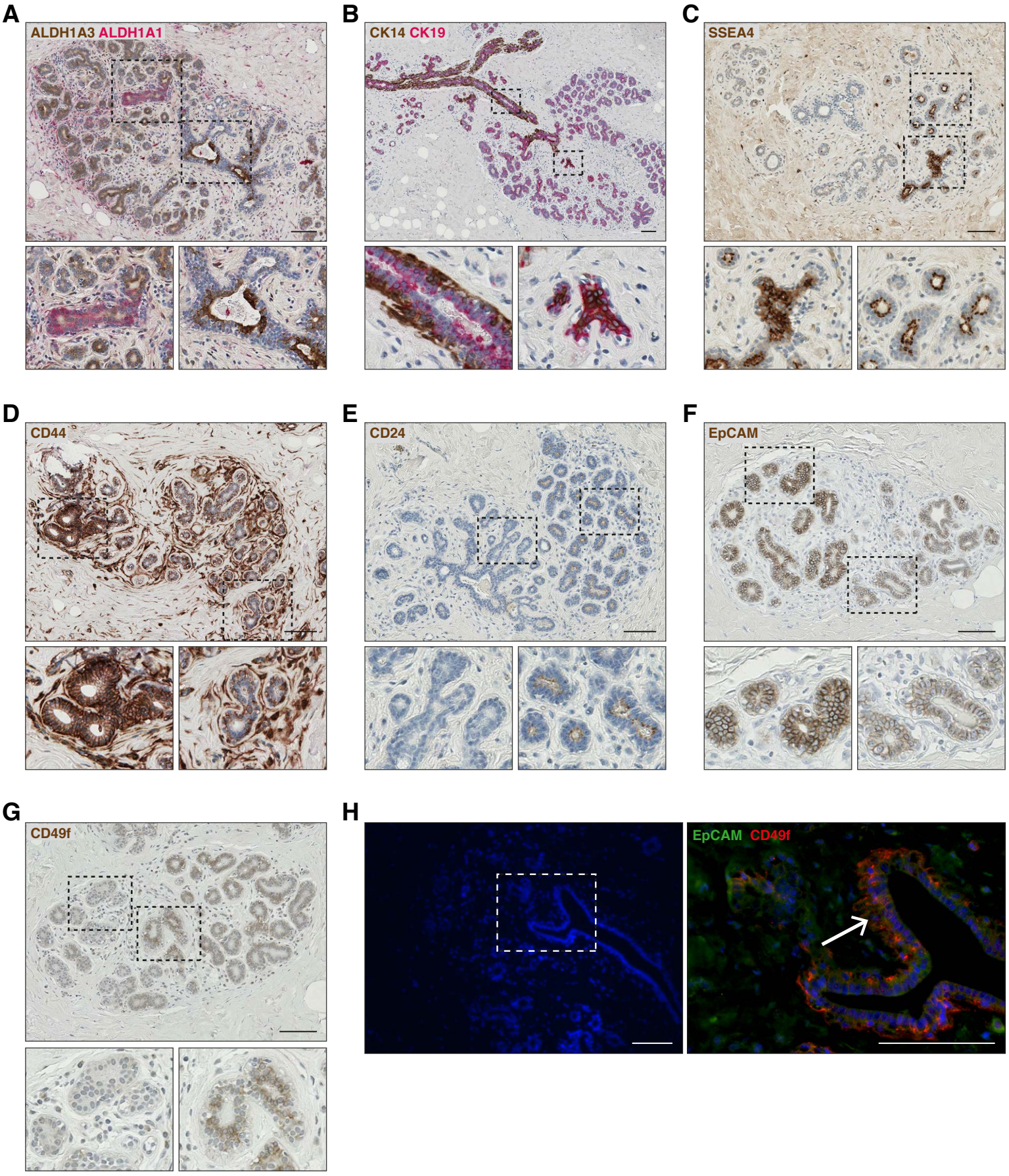
A
ALDH1A3 ALDH1A1
B
CK14 CK19
C
SSEA4
D
CD44
E
CD24
F
EpCAM
G
CD49f
H
EpCAM CD49f

FIGURE S3

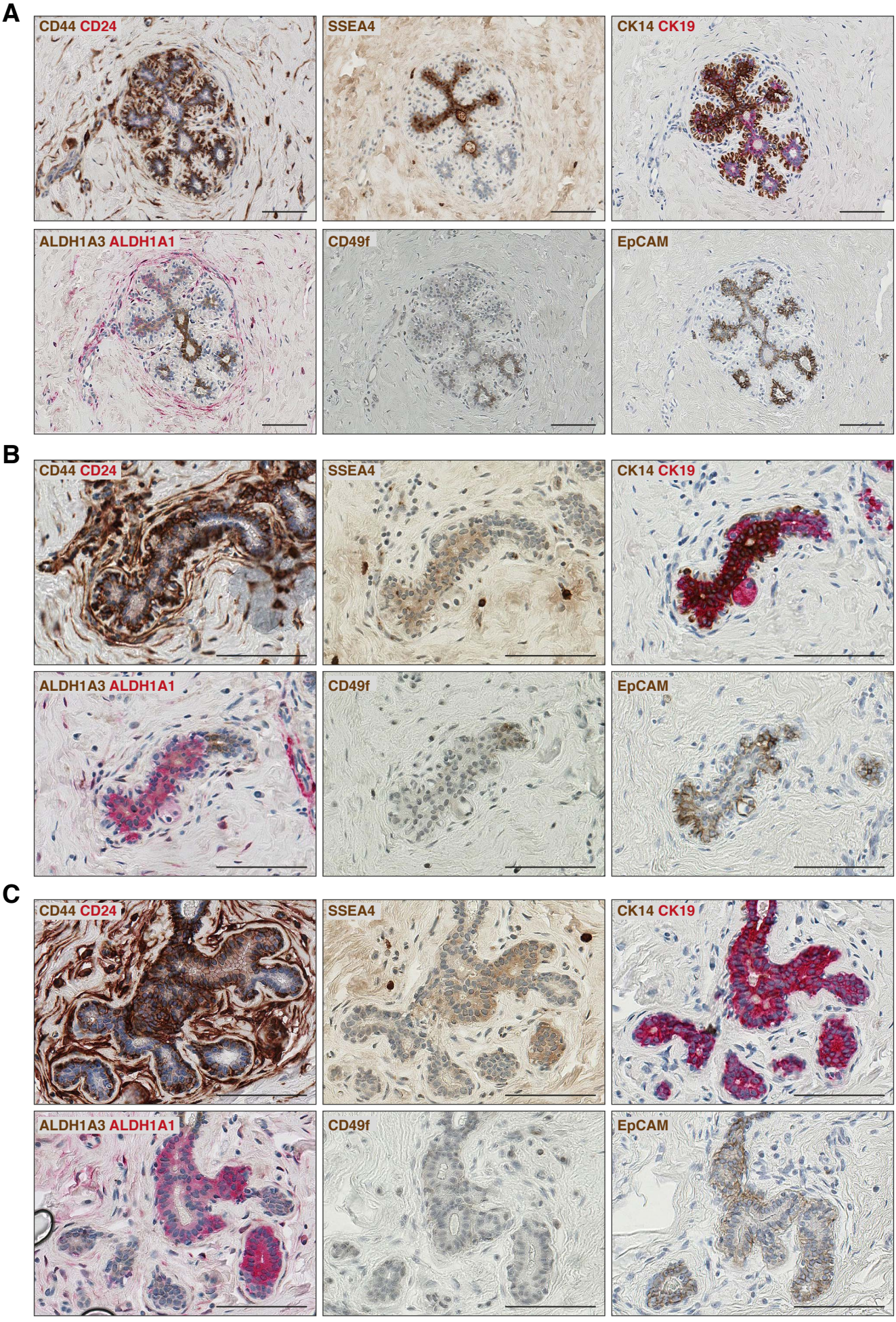
A
CD44 CD24
SSEA4
CK14 CK19
ALDH1A3 ALDH1A1
CD49f
EpCAM
B
CD44 CD24
SSEA4
CK14 CK19
ALDH1A3 ALDH1A1
CD49f
EpCAM
C
CD44 CD24
SSEA4
CK14 CK19
ALDH1A3 ALDH1A1
CD49f
EpCAM

FIGURE S4

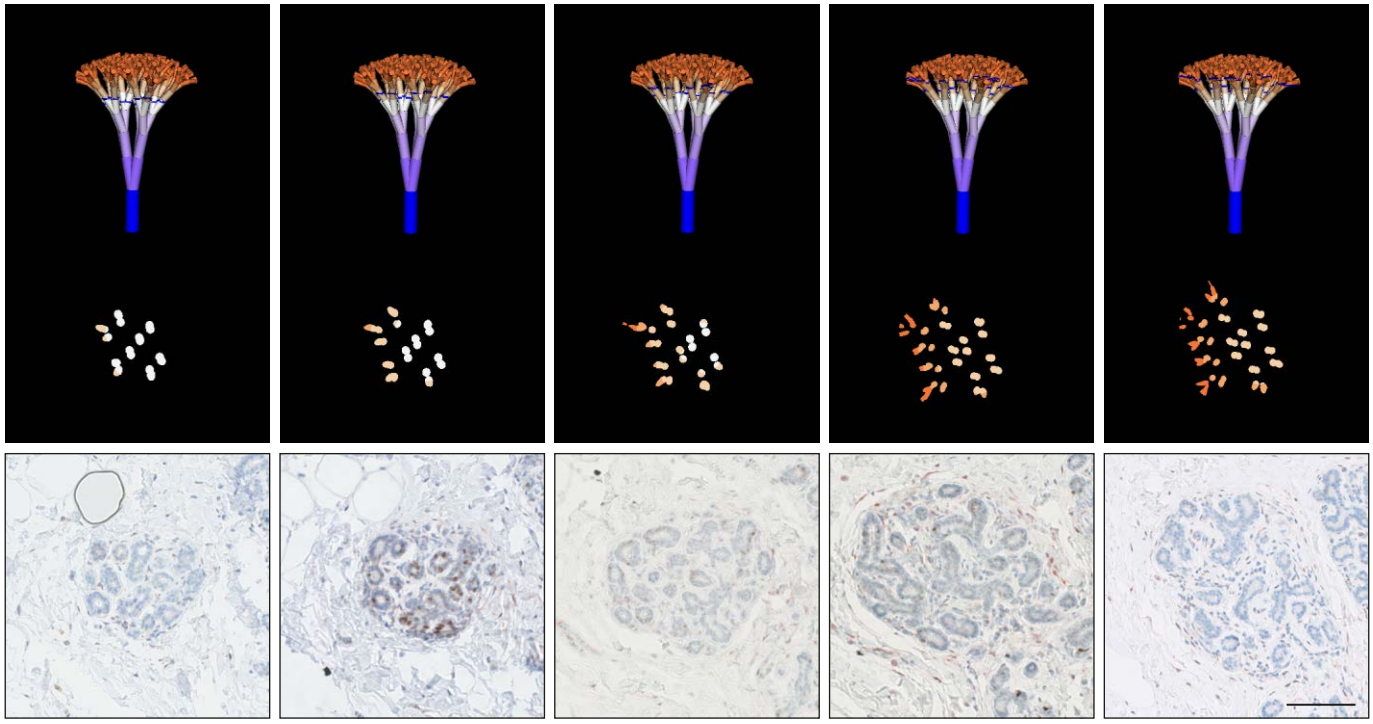

FIGURE S5

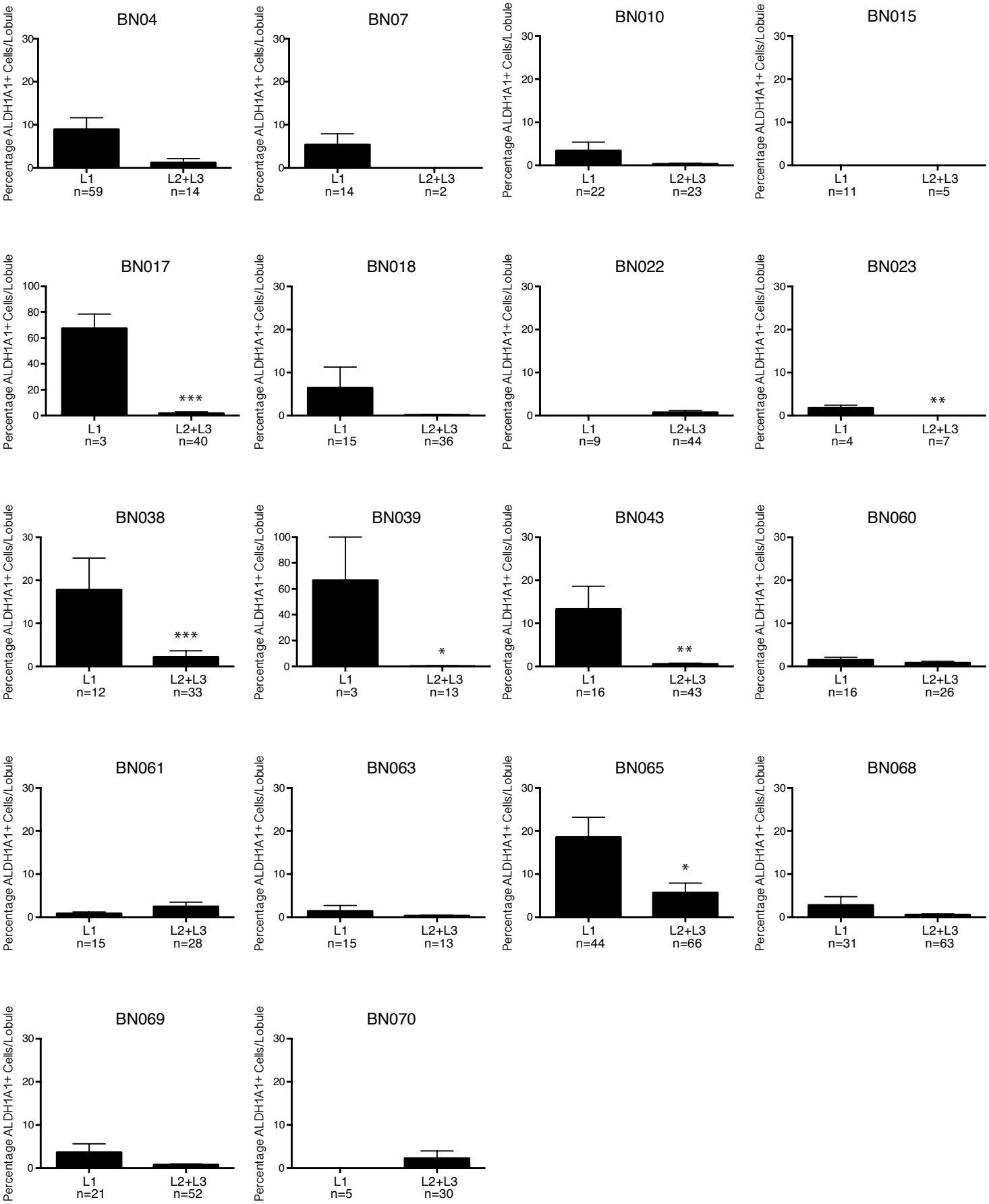
BN04
Percentage ALDH1A1+ Cells/Lobule
L1 n=59
L2+L3 n=14
BN07
L1 n=14
L2+L3 n=2
BN010
L1 n=22
L2+L3 n=23
BN015
L1 n=11
L2+L3 n=5
BN017
***
L1 n=3
L2+L3 n=40
BN018
L1 n=15
L2+L3 n=36
BN022
L1 n=9
L2+L3 n=44
BN023
**
L1 n=4
L2+L3 n=7
BN038
***
L1 n=12
L2+L3 n=33
BN039
*
L1 n=3
L2+L3 n=13
BN043
**
L1 n=16
L2+L3 n=43
BN060
L1 n=16
L2+L3 n=26
BN061
L1 n=15
L2+L3 n=28
BN063
L1 n=15
L2+L3 n=13
BN065
*
L1 n=44
L2+L3 n=66
BN068
L1 n=31
L2+L3 n=63
BN069
L1 n=21
L2+L3 n=52
BN070
L1 n=5
L2+L3 n=30

FIGURE S6

SUPPLEMENTAL FIGURE LEGENDS

Figure S1. Theoretical one-dimensional models of mammary lobule development based on cell fate decisions (Related to Figure 1)

(A) Schematic drawing of the mammary ductal tree, illustrating the difference in size between lobules type 1, 2 and 3.

(B) In situ sections through normal human breast, stained with hematoxylin and eosin, showing cross-sections through the three types of lobules. Scale bar = 100 μm.

(C) Summary of cell fate choices taken into consideration when generating the theoretical models shown in D-F.

(D) Theoretical one-dimensional models for mammary lobule development. For each model, four generations of cell divisions are shown (indicated in lines of cells from top to bottom). Colors of cells indicate differentiation status, with darker color being more undifferentiated cells (dark red/brown = stem cells, dark pink = first generation of daughter cells, light pink = second generation of daughter cells, grey = third generation of daughter cells, white = forth generation of daughter cells and beyond). Numbers on cells indicate if they are identical daughters. Symmetric division (example shown in F) would generate cells with the same number, while asymmetric division generates cells with different numbers. Cells with the same number belong to the same generation and fate. Q indicates the quiescent stem cells. Combination of stem cell fate choices summarized in C, generate the eight different models shown in D. These models predict rate of growth and differentiation as well as representation and localization of stem cells in the growing lobule. Two examples of these models are also shown in more detail in main Figure 1.

(E) Example of a variant of the model combining asymmetric self-renewal, high rate of division and distal orientation (A1B2C1) where one symmetric self-renewal of stem cells followed by asymmetric self-renewal are additionally included in the model.

(F) Example of a variant of the model A1B2C1 where symmetric division of progenitor cells was modeled. The variants of A1B2C1 shown in E and F do not change the predictions of this model in a way that could be verified by IHC analysis. These cell fate choices were not considered further.

Figure S2. Expression patterns of proliferation and differentiation markers in normal breast epithelium (Related to Figure 1)

In situ staining patterns of proliferation marker MCM2, estrogen receptor (ER), myoepithelial markers CD10 and SMA, and luminal markers EpCAM and CK18 in sections through normal human breast. Scale bar = 100 μm.

Figure S3. Expression patterns of putative stem cell markers in normal breast epithelium (Related to Figure 2)

(A) Double staining for ALDH1A1 (red) and ALDH1A3 (brown) in the normal breast. ALDH1A1 was detected in distinct islands in the lobule (left insert) while high level ALDH1A3 was detected in the luminal layer of interlobular as well as larger extralobular

ducts (right insert). Lower level ALDH1A3 was detected in the luminal layer of lobules (these cells are not detected by ALDEFLUOR). Cells completely negative for ALDH1A3 were often found next to the strongly positive cells in intralobular ducts. ALDH1A1 and ALDH1A3 markers never co-localized. The staining patterns for ALDH1A1 and ALDH1A3 were very consistent between samples.

(B) Double staining for CK14 (brown) and CK19 (red) in the normal breast. CK19 was detected in the vast majority of luminal cells in both ducts and lobules. CK14 was expressed in the basal cell layer of large and intermediate ducts (left insert), but generally not within the lobules. In rare but very distinct clusters within the lobules, CK14 was expressed in the luminal layer and overlapping with CK19 (right insert).

(C) Staining for SSEA4 (brown) in the normal breast. SSEA4 was detected in the cytoplasm of distinct islands of the luminal layer in lobules (left insert). In this particular sample we also detected high-level apical SSEA4 staining in some lobules (right insert).

(D) Staining for CD44 (brown) in the normal breast. CD44 was detected in the membrane of cells mainly in the basal layer (right insert, low level staining) and occasionally also in the luminal layer (left insert, high level staining).

(E) Staining for CD24 (brown) in the normal breast. CD24 was occasionally detected in the luminal layer, predominantly in apical localization (right insert). CD24 positive cells were not detected in all mammoplasty samples. Left insert shows an area negative for CD24.

(F) Staining for EpCAM (brown) in normal breast sections. EpCAM was detected in the membrane of the majority of cells in the luminal layer throughout ducts and lobules, at different levels of intensity (left insert show high level and right insert show low level). Rare negative areas could also be seen.

(G) Staining for CD49f (brown) in normal breast sections. CD49f was detected at different levels throughout the epithelium. Inserts show areas negative (left) and positive (right), respectively.

(H) Double IF staining for EpCAM (green) and CD49f (red). Blue is nuclear DAPI staining. Right image is higher magnification of the area marked in the left image. CD49f+EpCAM– cells is seen in basal localisation in large ducts (arrow).

Each marker was evaluated on at least six different mammoplasty samples and the staining patterns shown are representative. Scale bar = 100 μm.

Figure S4. Putative stem cell markers co-localize in the normal breast epithelium (Related to Figure 2)

(A) Representative area of normal breast epithelium corresponding to an immature lobule emerging from parental secondary duct. SSEA4+, CK14+CK19+ and ALDH1A1+ markers co-localize in this area. CD49f is not expressed in this area and EpCAM is expressed at moderate level.

(B) Representative area showing a branching point where CD44+, SSEA4+, CK14+CK19+ and ALDH1A1+ markers co-localize. CD49f is not expressed in this area and EpCAM is expressed at moderate level.

(C) Representative area of a type 1 lobule where CD44+, SSEA4+, CK19+ and ALDH1A1+ markers co-localize. CD49f is not expressed in this area and EpCAM is expressed at moderate level. Higher levels of SSEA4 are seen in A due to intense apical staining, not seen in B and C (see also Figure S3C). Scale bar = 100 μm.

Figure S5. Comparison of virtual and real consecutive sections through a mammary lobule (Related to Figure 4)
Multiple cross-sections through a fractal tree with corresponding consecutive sections through a mammary lobule.

Figure S6. Representation of ALDH1A1 in mammary lobules in individual samples (Related to Figure 5)
Quantitative analysis of ALDH1A1+ cells representation in lobules type 1-3 for the 18 different mammoplasty samples included in the study shows that the majority of samples (14 out of 18) show the same trend of higher percentage of ALDH1A1+ cells in lobules type 1 compared with lobules type 2 and 3. This difference was statistically significant for six of the samples. The remaining four samples show no difference or a very slightly higher percentage (not statistically significant) in lobules type 2-3. Bars represent mean percentage ALDH1A1+ cells ± SEM. P values were calculated using Mann-Whitney U test. *p≤0.05; **p≤0.01, ***≤0.001.

SUPPLEMENTAL EXPERIMENTAL PROCEDURES

Clinical Characteristics of Patients Included in the Study

Patient	Age	Menopause status	Parity#	Type of Surgery	BC History*
BN004[1,2,3]	21	Premenopausal	Nulliparous	Bilateral Breast Reduction	None
BN007[3]	34	Therapy Induced Menopause	Parous	Left Mastectomy	Contralateral IDC (Age 33)
BN010[2,3]	28	Premenopausal	Nulliparous	Bilateral Breast Reduction	None
BN015[3]	44	Oopherectomy (Age 44)	Parous	Left Risk Reducing Mastectomy	Contralateral IDC (Age 39)
BN017[1,2,3]	24	Premenopausal	Nulliparous	Bilateral Risk Reducing Mastectomy	None (BRCA2 Carrier)
BN018[3]	38	Premenopausal	Nulliparous	Left Mastopexy	Contralateral IDC (Age 33)
BN022[3]	40	Chemotherapy Induced Menopause (Age 40)	Parous	Right Risk Reducing Mastectomy	Concurrent Contralateral IBC
BN023[3]	46	Postmenopausal	Parous	Right Risk Reducing Mastectomy	Contralateral BC (Age 44)
BN024[1]	16	Premenopausal	Nulliparous	Bilateral Breast Reduction	None
BN027[2]	43	Premenopausal	Nulliparous	Bilateral Breast Reduction	None

BN037[4]	41	Chemotherapy Induced Menopause (Age 41)	Parous	Left Mastectomy	Concurrent Contralateral BC (BRCA1 Carrier)
BN038[1,3]	43	Hysterectomy (Age 40)	Parous	Left Risk Reducing Mastectomy	Concurrent Contralateral Invasive BC (BRCA2 Carrier)
BN039[1,3]	43	Chemotherapy Induced Menopause (Age 43)	Parous	Risk Reducing Mastectomy	Concurrent Contralateral BC (BRCA2 Carrier)
BN041[4]	41	Premenopausal	Parous	Left Breast Reduction	Concurrent Contralateral BC
BN043[2,3,4]	42	Premenopausal	Parous	Bilateral Risk Reducing Mastectomy	None (BRCA1 Carrier)
BN044[4]	40	Premenopausal	Nulliparous	Bilateral Mastopexy	None
BN049[4]	54	Chemotherapy Induced Menopause (Age 47)	Parous	Risk Reducing Mastectomy	Contralateral BC (Age 45)
BN050[4]	33	Premenopausal	Parous	Right Risk Reducing Mastectomy	Concurrent Contralateral DCIS
BN055[2,4]	40	Premenopausal	Parous	Bilateral Risk Reducing Mastectomy	None (BRCA2 Carrier)
BN059[4]	50	Postmenopausal	Parous	Risk Reducing Mastectomy	None (BRCA2 Carrier)
BN060[2,3,4]	18	Premenopausal	Nulliparous	Bilateral Breast Reduction	None
BN061[2,3,4]	45	Premenopausal	Parous	Bilateral Breast Reduction	None
BN062[4]	45	Premenopausal	Nulliparous	Bilateral Breast Reduction	None
BN063[3,4]	29	Premenopausal	Parous	Bilateral Risk Reducing Mastectomy	None (BRCA2 Carrier)
BN064[4]	46	Premenopausal	Nulliparous	Right Risk Reducing Mastectomy	Concurrent Contralateral Lobular Carcinoma
BN065[1,3,4]	44	Premenopausal	Parous	Bilateral Risk Reducing Mastectomy	None (BRCA2 Carrier)
BN067[4]	46	Premenopausal	Parous	Bilateral Breast Reduction	None
BN068[3,4]	42	Oopherectomy (Age 42)	Parous	Bilateral Risk Reducing Mastectomy	None (BRCA1 Carrier)
BN069[3,4]	36	Premenopausal	Parous	Left Risk Reducing Mastectomy	Concurrent Contralateral DCIS
BN070[3,4]	36	Premenopausal	Parous	Left Risk Reducing Mastectomy	Concurrent Contralateral Invasive BC (BRCA2 Carrier)

BN071[4]	60	Postmenopausal	Nulliparous	Bilateral Breast Reduction	None
BN072[4]	53	Postmenopausal	Parous	Bilateral Risk Reducing Mastectomy	None (BRCA1 Carrier)
BN073[4]	37	Chemotherapy Induced Menopause (Age 37)	Parous	Right Risk Reducing Mastectomy	Concurrent Contralateral BC
BN074[4]	49	Hysterectomy (Age 47)	Parous	Bilateral Risk Reducing Mastectomy	None (BRCA2 Carrier)
BN075[4]	28	Premenopausal	Parous	Right Breast Reduction	None

[1] Used for immunostainings of series of markers on consecutive stainings
[2] Stained with immunofluorescence
[3] Included in lobule analysis
[4] Included in mammosphere analysis
[#] Women were considered parous if at least one pregnancy progressed past the first trimester. Otherwise they were considered nulliparous.
* BC=Breast Cancer; DCIS=Ductal Carcinoma In Situ; IBC=Inflammatory Breast Cancer; IDC=Invasive Ductal Carcinoma

Antibodies Used for Immunostainings

Antigen	Conjugate	Clone	Company	Source	Dilution	Antigen Retrieval
ALDH1A1		44/ALDH	BD Biosciences	mouse	1:50	Heat Induced, pH6
ALDH1A1		EP1933Y	Abcam	rabbit	1:200	Heat Induced, pH6
ALDH1A3		C-13	Santa Cruz	goat	1:200	Heat Induced, pH6
CD10		56C6	Novocastra	mouse	1:100	Heat Induced, pH6
CD24		SN3b	NeoMarkers	mouse	1:50	Heat Induced, pH6
CD44		156-3C11	NeoMarkers	mouse	1:200	Heat Induced, pH6
CD49f			Atlas	rabbit	1:100	Heat Induced, pH9
CK14		LL002	Dako	mouse	1:50	Heat Induced, pH6
CK14	FITC	LL002	Abcam	mouse	1:20	Heat Induced, pH6
CK18		DC-10	Novocastra	mouse	1:20	Heat Induced, pH6
CK19		A53-B/A2	Abcam	mouse	1:200	Heat Induced, pH6
EpCAM		VU-1D9	Novocastra	mouse	1:25	Trypsin
EpCAM	FITC	VU-1D9	StemCellTech	mouse	1:5	Heat Induced, pH9
ER		EP1	Dako	rabbit	1:100	Heat Induced, pH6
MCM2		CRCT2.1	Novocastra	mouse	1:50	Heat Induced, pH6
p27		SX53G8	Dako	mouse	1:25	Heat Induced, pH6
SMA		HHF35	Novocastra	mouse	1:100	Heat Induced, pH6
SSEA4		MC-813-70	Millipore	mouse	1:50	Heat Induced, pH6

Theoretical Parameters Used in Modeling Cell Divisions during Branching Morphogenesis (One-Dimensional Modeling)

Definitions:

Stem cells**:** Cells capable to: a) differentiate and generate all types of differentiated cells present in the mammary lobule, and b) self-renew and generate progenies identical to themselves. We acknowledge that these may be the most undifferentiated cells in the lobule rather than the most primitive cells in the entire mammary gland.

Progenitor cells**:** Any cells that can proliferate.

Differentiated cells (or terminally differentiated cells)**:** Postmitotic cells with no proliferation potential.

Branching points: The areas of dichotomic split within a lobule.

Branching generation: 0 = no split; 1 = one dichotomic split, two branches; 2 = two dichotomic splits, four branches; 3 = four dichotomic splits, eight branches; etc.

Assumptions:

1. Branching morphogenesis in the lobule is dichotomic.
2. Stem cells can be quiescent.
3. Progenitor and differentiated cells proliferate until terminal differentiation (modeling of mature pre-menopausal lobule, outside pregnancy, lactation, involution).
4. Cellular de-differentiation is not a common phenomenon in the normal adult breast tissue.

Cell Fates Taken in Consideration:

1. Type of cell divisions
    a. *Self-renewal cell division* – A cell division that generates a daughter cell identical to the mother cell. This cell will have the same proliferation potential as the mother cell, but may occupy a different position.
    OR
    b. *Differentiating cell division* – A cell division that generates daughter cells different from the mother cell, with increasingly lower proliferation potential. After a finite number of differentiating divisions, terminally differentiated cells with no ability to proliferate are generated.
2. Symmetry of cell divisions (both self-renewal and differentiating divisions can be symmetric or asymmetric)
    a. *Symmetric cell division* – A cell division that generates identical daughter cells
    OR
    b. *Asymmetric cell division* – A cell division that generates two distinct progenies

3. Location of cells
    a. *Proximal* – more undifferentiated daughter cell close to parental duct OR
    b. *Distal* – more undifferentiated daughter cell away from parental duct

Excluded Parameters:

1. Cell death.
2. Only luminal cells are shown in the diagrams. Myoepithelial cells form an outer layer, relatively uniform in phenotypic markers. They are not shown in order to simplify the diagrams. The addition of myoepithelial cells does not change the types of morphogenesis predicted.
3. Proliferation and differentiation driven by extrinsic factors (steroid hormones, growth factors, etc.). The growth of the lobule may be halted and re-started depending on levels of these hormones during the menstrual cycle.
4. Feedback and feed-forward signaling between cells with impact on differentiation or proliferation.
5. Mechanical forces with impact on differentiation or proliferation.
6. Development of the lobules during pregnancy, lactation and involution.

Experimental Parameters for Fractal Model Generation

These parameters were measured in tissue sections through normal breast, by measuring ductules in type 3 lobules (classified as described in Experimental Procedures). A total of 12 lobules cut longitudinally from three different mammoplasty samples were analyzed for ductule length. An average of 5 ductules/lobule were measured. For ratio, consecutive ductules (where two branching points were clearly visible) were measured. A total of 9 lobules cut transversally, from three mammoplasty samples were analyzed for duct diameter. Angle measurements were done in longitudinally cut lobules.

1. Length of first ductule in the mature type 3 lobule: 300 μm or 58 cells in circumference
2. Diameter of first ductule in the mature type 3 lobule: 100 μm or 32 cells in circumference
3. Ratio length: 0.794
4. Ratio diameter: 0.858
5. Rotation angle: 60

Variable parameters:

- Number of branching generations (number of times the ductules branched)
- Angle of branching

Fractal Modeling of Lobule Formation

We simulated the growth of breast ducts using a fractal approach, drawing heavily upon work done using L-systems to model the growth of tree-like structures.

In our idealized model, we assumed that every breast duct originates from a single trunk, which branches in two and creates two self-similar structures of reduced size.

The model is made of a set of *ducts* (D), each duct starts from a *branching node* (*node* for short) and ends into another one. A duct is *parent* of the ducts (*children*) spawning from its ending node. Similarly we can indicate such an ending node as parent of the ending nodes of the two children ducts.

The model is governed by multiple parameters and initial conditions:

- **L**: the length of the stem (initial duct)
- **R**: the radius of the stem
- **n**: the number of levels of the model
- **ϱ**: the ratio between parent and children thickness (radius)
- **λ**: the ratio between parent and children length
- **β_i**: the angle of branching between two children ducts at level **i** (i=0,1...,n); β_0 sets the direction of the stem: $\pi/2$ (the plane described by the two branching ducts is their branching plane)
- **α**: the polar angle determining the rotation of the children branching plane with respect to the parent branching plane

All angels can be changed for all levels of branching, which provides a higher flexibility in modelling.

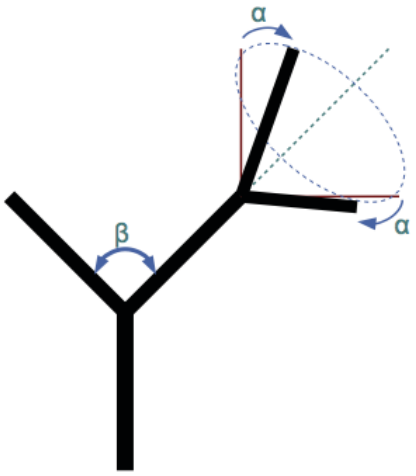

Figure: The role of α and β in the creation of the tree. The angle of dichotomic branching is designated β. The rotation of children branches around the parent axis (in red the branches before rotation) is measured by rotation angle α.

Parameters and initial conditions were obtained as described above.

The simulations are implemented in Python using simple mathematical formulas (code available upon request). The rendering of the trees is done using the VTK package for Python (courtesy of Enthought, INC) using custom written software.

For each set of parameters, we can generate a duct structure, then slice the duct structure at an arbitrary depth and angle.

We note that the system is fully deterministic, and produces a perfectly symmetric idealized duct structure. Still, even with these simplifications, the structures produced by our model closely resemble structures seen in situ in cross-sections through the breast.

Model Fitting

Fractals were generated by giving values between 3 and 12 for number of branching generations and constant or variable angles of branching between 15-120°. The angles are affected by the angle of the section plane with the three axes of the lobule and may not correspond to the real branching angle.

At the 12th branching generation, the ductule is formed of only 4 cells, and cannot grow following the same ratio as the rest of the fractal tree. Duct ends of 4 and 3 cells can be found in breast tissue sections.

Sections through fractals were compared to tissue sections through lobules 1, 2 and 3. Transversal sections were preferentially analyzed. Additionally, angled sections were generated by changing stem inclination, stem rotation and tree rotation (the three axes of the lobule).

The following criteria were used to compare sections through the computer generated fractal tree to those seen in breast tissue sections. The comparisons were used to eliminate and refine parameters for computer modeling:

1. Maximum diameter of fractal tree (lobule)
2. Total number of ductule sections at maximum number of branches
3. Angles of branching at which ductules contacted each other were eliminated
4. Shape, size and pattern distribution of ductules in sections through fractal tree
5. Angles at which the ductule disposition was different from that observed in situ were eliminated (i.e. center of lobule with lower or higher density of ductules than observed in tissue sections or longitudinal sections in addition to cross sections, in a pattern not seen in tissue sections)

The parameters that modeled best the lobule in situ were variable angle of branching increasing from 15 to 70°.

Instructions to Use the Software "Ducts"

The software (Windows and Mac versions) can be downloaded from the following link: https://github.com/FedericoV/FractalMammaryLobule

To use the software:

1. The file "Ducts" will open the following window:

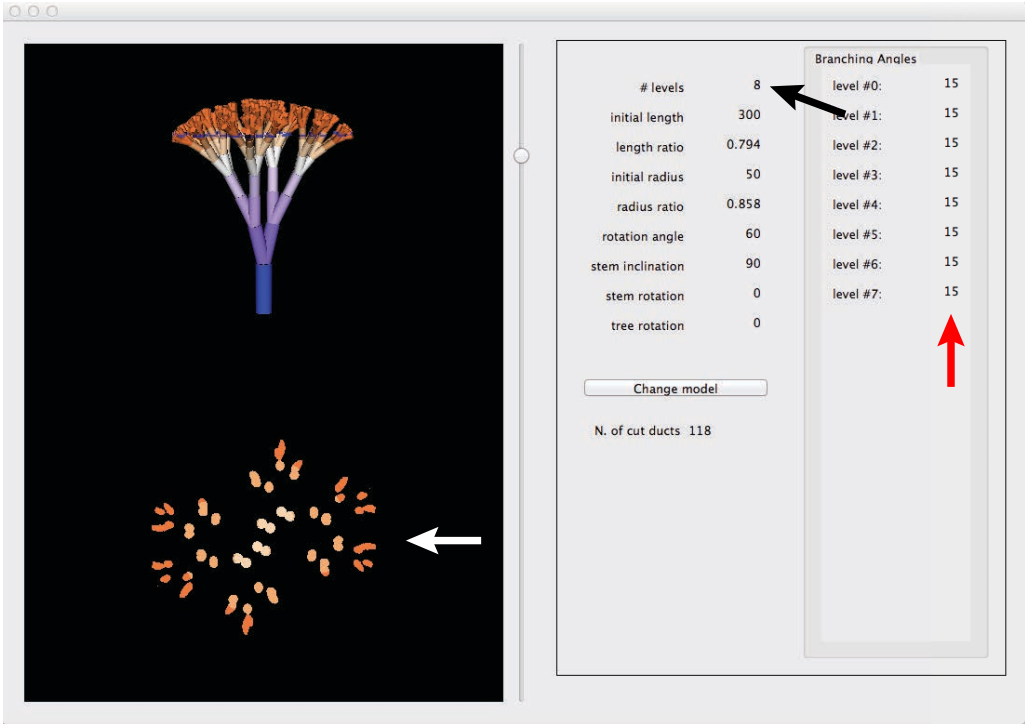

2. Assign the desired parameters (click "Change model" to be able to make changes). For instance in order to model eight dichotomic branching generations (levels) starting from the unique blue duct shown in the window, type 8 in the field # levels (black arrow).
3. Similarly assign the size of the ductule the modeling starts with (300 μm in length and 50 μm in radius in our modeling). The length ratio and radius ratio, between lengths of branches in consecutive generations are 0.794 and respectively 0.858 in our model (see above). The rotation of emerging branches (rotation angle) in the z axis is 60°.
4. The angle of branching can be changed for each branching generation (level) (red arrow).
5. To generate a cross-section click on the cursor at the right side of the image and drag to the desired position. The image of lobule in cross-section will appear at the bottom of the 3D image (white arrow).
6. To zoom in and out left click on the 3D image and use the mouse wheel. Both 3D image and cross-section will zoom. To rotate the 3D image right-click and move the mouse.
7. To change the angle of the cross-section, change the value for stem inclination. In the figure below the stem inclination is changed to 45° (arrowhead), compared to 90° in the picture above.

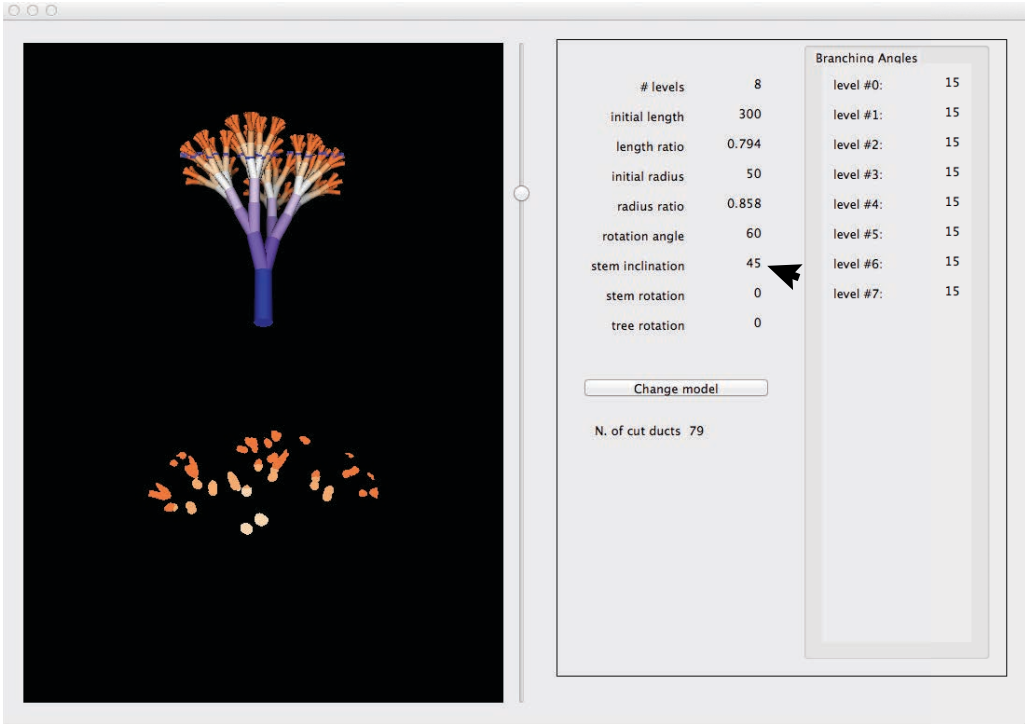
levels 8
initial length 300
length ratio 0.794
initial radius 50
radius ratio 0.858
rotation angle 60
stem inclination 45
stem rotation 0
tree rotation 0
Change model
N. of cut ducts 79
Branching Angles
level #0: 15
level #1: 15
level #2: 15
level #3: 15
level #4: 15
level #5: 15
level #6: 15
level #7: 15